at depolarized and hyperpolarized potentials. The smoothed amplitude distribution histograms of responses and noise were generated as described [R. Malinow, *Science* **252**, 722 (1991)]. The peak at zero amplitude represents failures of synaptic transmission and matched the amplitude distribution of the noise (mean ± SD: 0.82 ± 0.07 pA at −60 mV and 0.90 ± 0.09 pA at +55 mV; $n$ = 16). The rate of failures was measured by doubling the fraction of responses with amplitudes less than zero (*7*). The failure rates at depolarized ($F_d$) and hyperpolarized ($F_h$) potentials are approximated by $F_h = (1 - Pr)^{nAN}$ and $F_d = (1 - Pr)^{(nAN + nN)}$, where $n_{AN}$ is the number of releasing sites producing AMPA responses and $n_N$ is the number of releasing sites producing only NMDA responses. *Pr* is the probability of release and is assumed to be similar in both kinds of synapses given that a 15-fold change in probability of release does not appreciably change the AMPA/NMDA ratio [D. J. Perkel and R. A. Nicoll, *J. Physiol.* **471**, 481 (1993)]. (A similar calculation for failure rate is obtained if a heterogeneous, rather than a single, probability of release is assumed.) Rearrangement yields the fraction of pure NMDA responses: $n_N/(n_{AN} + n_N) = 1 - (\ln F_h/\ln F_d)$. The difference in failure rate at −60 mV and at +55mV was eliminated by 100 μM APV (failure rate at hyperpolarized potentials = 0.55 ± 0.08, at depolarized potentials = 0.23 ± 0.07, and at depolarized potentials with APV = 0.54 ± 0.09; $n$ = 4). Pure NMDA responses can be attributed to the existence of synapses with only functional NMDA receptors (*7–9*). It is unlikely that the absence of AMPA responses at some synapses is due to greater electrotonic filtering of the faster AMPA response, because immature cells are more compact and yet have more, not less, synapses with only NMDA responses (Fig. 4G).


31. G. Carmignoto and S. Vicini, *Science* **258**, 1007 (1992).
32. S. Hestrin, *Nature* **357**, 686 (1992).
33. Vaccinia virus constructs (*20*) were injected into the brain ventricle of stage 44 to 45 tadpoles (*22*). Three days later, when the animal was at stage 47 to 48, the brain was dissected and used for recordings. Animals infected at the same time were stained in wholemount with X-Gal to test for β-Gal expression. Infection of amphibian cells with vaccinia virus does not result in decreased cell density (*14*, *22*), arguing against a cytotoxic action of the virus in this species.
34. D. Liao and R. Malinow, *Learn. Mem.*, in press.
35. K. Fox, H. Sato, N. Daw, *J. Neurosci.* **9**, 2443 (1989).
36. M. C. Crair and R. C. Malenka, *Nature* **375**, 325 (1995).
37. Only two cells had all evoked responses mediated by only NMDA receptors. This paucity can be explained if a single axon makes a number of contacts onto each postsynaptic cell. The gradual change in fraction of pure NMDA responses across the RC axis then reflects addition of AMPA receptor function to individual contacts already showing NMDA receptor function. An alternative interpretation is that pure NMDA responses are due to spillover of transmitter from nearby synapses. In this instance, during development there must be a decrease in spillover (to account for the lower fraction of pure NMDA responses) and a compensating increase in probability of release (to maintain NMDA transmission constant). Furthermore, postsynaptic increase in CaMKII must also decrease spillover and increase probability of transmitter release (to explain similar changes in caudal cells infected with tCaMKII-VV). However, rostral cells infected with tCaMKII-VV showed no change in failure rates (either hyperpolarized or depolarized) (*26*), further arguing against this spillover model. Rostral cells infected with tCaMKII-VV did show an increase in AMPA receptor transmission with little change in NMDA receptor transmission. This result likely reflects the fact that rostral neurons in these animals continued to develop throughout the tadpole stage of development.
38. H. T. Cline, *Trends Neurosci.* **14**, 104 (1991).
39. Sources of the depolarization in the most caudal region of tectum, where the neurons have predominantly NMDA responses, could be intrinsic membrane oscillations or depolarizing GABAergic inputs [E. Cherubini, J. L. Gaiarsa, Y. Ben Ari, *Trends Neurosci.* **14**, 515 (1991)].


40. Supported by the NIH (R.M.), and the National Science Foundation, NIH, and National Down Syndrome Society (H.T.C.). We thank J. Lisman for comments on the manuscript, and members of the labs for helpful discussions.

14 June 1996; accepted 18 September 1996


# Distinct Mechanisms for Synchronization and Temporal Patterning of Odor-Encoding Neural Assemblies


Katrina MacLeod and Gilles Laurent*



**Stimulus-evoked oscillatory synchronization of neural assemblies and temporal patterns of neuronal activity have been observed in many sensory systems, such as the visual and auditory cortices of mammals or the olfactory system of insects. In the locust olfactory system, single odor puffs cause the immediate formation of odor-specific neural assemblies, defined both by their transient synchronized firing and their progressive transformation over the course of a response. The application of an antagonist of ionotropic γ-aminobutyric acid (GABA) receptors to the first olfactory relay neuropil selectively blocked the fast inhibitory synapse between local and projection neurons. This manipulation abolished the synchronization of the odor-coding neural ensembles but did not affect each neuron's temporal response patterns to odors, even when these patterns contained periods of inhibition. Fast GABA-mediated inhibition, therefore, appears to underlie neuronal synchronization but not response tuning in this olfactory system. The selective desynchronization of stimulus-evoked oscillating neural assemblies in vivo is now possible, enabling direct functional tests of their significance for sensation and perception.**


Although stimulus-evoked oscillatory synchronization of neuronal assemblies has been observed in many sensory systems (*1–3*), the mechanisms (cellular, synaptic, and network) underlying coherent recruitment of neurons still remain elusive (*4*). Consequently, it has not yet been possible to selectively alter or suppress the synchronization of such assemblies in vivo, a step essential to test their functional significance for neural coding. The possible functions (if any) of neural synchronization thus remain largely unknown. In the vertebrate olfactory system, bursts of odor-evoked γ (30 to 60 Hz) oscillations ("induced waves") can be seen in the olfactory bulb electroencephalogram during each respiratory cycle (*5*). Induced waves are generated within the bulb (*1*) and have been postulated to result from negative-feedback interactions between granule and mitral cell populations (*6*).

Odor-evoked synchronization of firing has been observed also in the locust *Schistocerca americana* (*7*). In the locust, odors puffed on an antenna cause the synchronization of groups of antennal lobe projection neurons (PNs) (the functional analogs of vertebrate olfactory bulb mitral-tufted cells), resulting in 20- to 30-Hz local field potential (LFP) oscillations in the mushroom body (the functional analog of the piriform cortex) and in subthreshold oscillatory responses in its intrinsic neurons, the Kenyon cells (KCs) (*7*). Although odor puffs evoke long oscillatory LFP bursts, individual PNs generally participate in the synchronized ensembles only for short epochs, but at times that are both neuron- and odor-specific (*7*). The bursts of odor-evoked LFP oscillations therefore result from dynamic neural ensembles whose components (the PNs) phase-lock transiently to one another and change reliably during a single odor response (*2*, *7*). To assess whether the periodic neural synchronization results primarily from local feedback inhibition, as hypothesized for the vertebrate olfactory system (*6*), we studied directly the role of local neurons (LNs) in synchronizing groups of PNs in the antennal lobe of the locust olfactory system.

Intracellular labeling of local neurons (*8*) revealed extensive dendritic arbors throughout the entire antennal lobe neuropil, providing a potential morphological substrate for widespread synchronization (Fig. 1A). Simultaneous intracellular recordings were made from synaptically connected local and projection neurons in vivo ($n$ = 4 pairs) (Fig. 1B). They revealed that, during odor responses, the timing of the periodic depolarization in LNs corresponds precisely to that of the periodic hyperpolarization in postsynaptic PNs, and showed directly that LNs lead PNs by a quar-


California Institute of Technology, Biology Division, 139-74, Pasadena, CA 91125, USA.

*To whom correspondence should be addressed. E-mail: laurentg@starbase1.caltech.edu

ter period (96° ± 53°, mean ± SD; $n$ = 164 cycles), as predicted for olfactory bulb circuits (*9*). Injecting depolarizing current directly into individual LNs evoked sustained inhibition in postsynaptic PNs (Fig. 1C). Transmitter release from LNs was spike independent (*10*) and graded (*11*). Hyperpolarizing one LN never abolished the periodic inhibition of a postsynaptic PN during an odor response (*11*). Hence, the periodic inhibition of any one PN during an odor response must result from converging inhibitory input from many LNs. This can be seen in Fig. 1B also, where the size of each periodic inhibitory postsynaptic potential (IPSP) in the PN (asterisks) was not closely correlated with that of the corresponding depolarization of the impaled presynaptic LN. Parallel studies with immunogold anti-GABA immunocytochemistry and electron microscopy revealed the existence of direct GABAergic contacts onto the dendrites of PNs in the antennal lobe (*12*).

To examine directly whether inhibition by LNs underlies the synchronized oscillatory responses of PNs, we injected picrotoxin (PCT, an antagonist of ionotropic GABA receptors) locally in the antennal lobe and mushroom body (*13*). We measured odor-evoked synchronization of activity before and after PCT injection in three ways: (i) from the power spectrum of LFPs recorded in the mushroom body (monitoring population oscillations); (ii) from autocorrelations calculated from antennal lobe PN membrane potential (monitoring single-cell oscillations); and (iii) from cross-correlations between PN membrane potentials and mushroom body LFPs (monitoring phase locking between antennal lobe and mushroom body) (*14*). Examples of the latter analysis and the raw data to which it was applied are shown in Fig. 2. In control conditions, odor puffs evoked a burst of LFP oscillations in the mushroom body, indicating oscillatory responses in odor-specific sets of antennal lobe PNs, of which one was recorded intracellularly (Fig. 2A). The transient synchronization between this PN and the LFP oscillations can be seen in a sliding cross-correlation (*14*), which represents the progressive change of the cross-correlation function during the odor response (Fig. 2A). The vertical stripes in the cross-correlation show that this PN was phase-locked to the LFP oscillations during an epoch of the ensemble response. The spacing between the stripes indicates the periodicity of the oscillation; their position relative to zero-time-lag indicates the phase of the two signals.

Pressure injection of PCT in the antennal lobe (*13*) abolished the LFP oscillations in the mushroom body (Fig. 2B), the periodic IPSPs caused in PNs by LNs (Fig. 2, A and B), and the periodic cross-correlation pattern between LFP and PNs (Fig. 2B) within a minute of the injection ($n$ = 6). PCT, however, never suppressed the response of PNs to odors that normally activated them (Fig. 2B). The suppression of odor-evoked LFP oscillations by PCT, therefore, resulted not from a silencing of the PNs, but most likely from their desynchronization, caused by the block of GABA-mediated inhibition. This was confirmed in each case by auto-correlation of the PN responses, showing that PCT suppressed the 20- to 30-Hz periodicity of their responses to odors (*11*). Bath application of PCT ($n$ = 26) had the same effects as local injection. Injection of the same volume of saline in the antennal lobe had no effect on the oscillatory

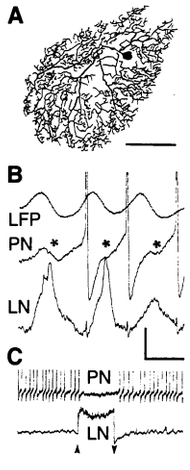


**Fig. 1.** Local neurons inhibit projection neurons monosynaptically. (**A**) Camera lucida drawing of a local neuron stained intracellularly from a dendrite by injection of cobalt hexamine. Dense, extensive arborizations occupy the entire neuropil, and no axon is present. Bar, 100 μm. (**B**) Simultaneous intracellular recordings from an antennal lobe local neuron (LN) and a postsynaptic projection neuron (PN), as well as the local field potential (LFP) from the ipsilateral mushroom body, during a response to a cherry odor in vivo. PN spikes are clipped. Calibrations: horizontal, 40 ms; vertical, 200 μV (LFP), 4 mV (PN), 5 mV (LN). (**C**) Direct current injection pulse (between arrowheads, 600 pA) in the LN [same pair as in (B)] inhibits tonic firing of PN (held depolarized by 300-pA constant current to evoke tonic spiking). The experiment was carried out in the absence of odor. The LN does not oscillate intrinsically upon depolarization. PN spikes are clipped. Calibrations: horizontal, 0.7 s; vertical, 32 mV (PN), 18 mV (LN).

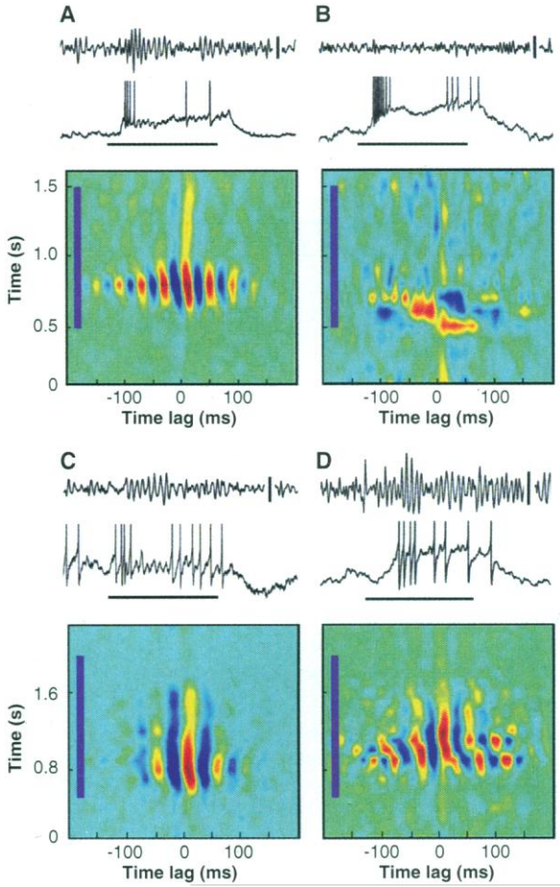


**Fig. 2.** Picrotoxin injection in the antennal lobe selectively abolishes the oscillatory synchronization but not the responsiveness of PNs. [(A) to (D)] (top trace) LFP from mushroom body; (middle) simultaneous intracellular recording from antennal lobe PN during odor puff (indicated by horizontal bar); (bottom) sliding cross-correlation between LFP and PN traces (*14*). Only the relative (and not the absolute) values of the cross-correlation functions matter. High values in hot colors, low values in cold colors. (**A**) Control response to mint odor. The biphasic PN response and the prominent IPSPs are apparent during the odor response. The oscillatory LFP indicates synchronized and rhythmic firing of many other PNs during the odor response. The cross-correlation between PN and LFP shows a striped pattern with ~50-ms period during the first half of the odor puff (vertical bar between 0.5 and 1.5 s), indicating an odor-evoked transient synchronization between this PN and the LFP (*14*). (**B**) Same pair as in (A), 2 min after pressure injection of 800 μM PCT into the antennal lobe. Although the response pattern of the PN to mint is not qualitatively altered (the periods of initial excitation, suppression, and subsequent excitation are preserved), the IPSPs have disappeared (indicating the block of LN-mediated fast inhibition), and the 20-Hz LFP oscillations are abolished. The cross-correlation is aperiodic, indicating desynchronization of the PN assembly representing mint. (**C**) Local injection of saline into the antennal lobe has no effect on synchronization and LFP oscillations, indicating that the manipulation per se does not disrupt the local circuits. A different animal was used from that in (A) and (B). (**D**) Local injection of PCT into the calyx of the mushroom body (where the axonal collaterals of PNs terminate) does not affect either the responsiveness of PNs to odors or their synchronization (assessed from the LFP oscillations or the periodic cross-correlation). [(A) to (D)] PN spikes are clipped. Calibrations (electrophysiological traces): horizontal, 1 s; vertical (in millivolts): LFP: [(A) and (B)] 0.2, (C) 0.5, (D) 0.3; PN: [(A) and (B)] 10, (C) 5, (D) 30.

synchronization (Fig. 2C) ($n$ = 4) (*15*), indicating that the integrity of the local circuits was not affected by the mechanical aspects of drug injection. Injection of PCT into the calyx of the mushroom body ($n$ = 6) also did not block the odor-induced LFP oscillations or the oscillatory responses of PNs (Fig. 2D), indicating that PN synchronization does not depend on inhibitory feedback in the mushroom body.

Immunocytochemical examination of synapses in the dendritic region of the mushroom body indicated that its intrinsic neurons, the KCs, receive direct GABA-containing inputs from neurons other than the PNs (*12, 16*). Inhibition in the mushroom body might thus also contribute to synchronization of the KCs receiving coherent inputs from PNs. To examine this idea, we superfused the brain with PCT, thus blocking inhibition both in the antennal lobe and the mushroom body, and monitored synchronization using the mushroom body LFP ($n$ = 17). A minute after PCT application, odor-evoked oscillations disappeared in the LFP because of the desynchronization of PNs in the antennal lobe (Fig. 3, A and B). A few minutes later, however, odor puffs evoked rhythmic bursts of large negative population spikes, indicative of massive synchronized firing of KCs (Fig. 3C). Power spectra of these oscillations showed that they occurred at the same frequency as control LFPs (*17*) (Fig. 3C). This result indicates that the mushroom body can naturally oscillate coherently at 20 to 30 Hz in response to a desynchronized input, and that inhibition may normally control the extent of this local synchronization. Examination of the KC axon tracts revealed reciprocal synapses that do not contain GABA and are therefore most likely excitatory (*12, 18*). Such recurrent excitation between neighboring KCs might participate in synchronizing their activity (*19*).

PNs generally respond to odors with complex temporal firing patterns that often include discrete periods of silence (*2, 7*). We assessed whether these slower temporal patterns, apparently sculpted by inhibition, also depend on PCT-sensitive inhibition in the antennal lobe. Two examples of PNs with such responses and of the effects of PCT on these responses are shown in Fig. 4. Although local injection (Fig. 4A) or bath application (Fig. 4B) of PCT at millimolar concentrations abolished the LN-mediated periodic IPSPs (arrowheads) and synchronized firing of the PNs (resulting in suppression of LFP oscillations), PCT had no qualitative effect on the temporal response patterns of the PNs (Fig. 4). Even though the LN-mediated IPSPs responsible for PN synchronization disappeared in PCT, the timing and duration of the PN responses remained unchanged and odor-specific, as seen both in intracellular responses and histograms of spike activity constructed from repeated presentations of an odor (Fig. 4) ($n$ = 17 PNs). The odor- and neuron-specific modulation of firing observed in PNs is therefore caused by mechanisms independent of PCT-sensitive GABA-mediated inhibition.

In conclusion, local neurons with extensive arbors monosynaptically inhibit projection neurons in the antennal lobe by way of fast, PCT-sensitive, GABA-containing synapses. This inhibition underlies the synchronization of ensembles of projection neurons and thus the odor-evoked LFP oscillations in the mushroom body. These results give experimental support to models of oscillatory synchronization proposed for the vertebrate olfactory bulb (*6, 20*) and neocortex (*21*) and extend evidence obtained in vitro from rat hippocampal slices (*22*). Fast inhibition in the locust antennal lobe does not, however, underlie the temporal response patterns expressed by individual PNs. Although slow-response patterns can also be observed in vertebrate mitral cells in vivo (*23*), it is not known whether they depend, as observed here, on synaptic mechanisms distinct from those causing synchronization. We also showed that the mushroom body is independently tuned to oscillate at 20 to 30 Hz. This probably enables it to "accept" the 20- to 30-Hz input from the antennal lobe. PCT-sensitive inhibition in the mushroom body appears to prevent stimulus-evoked runaway excitation that might otherwise result in seizures and, probably, loss of input specificity.

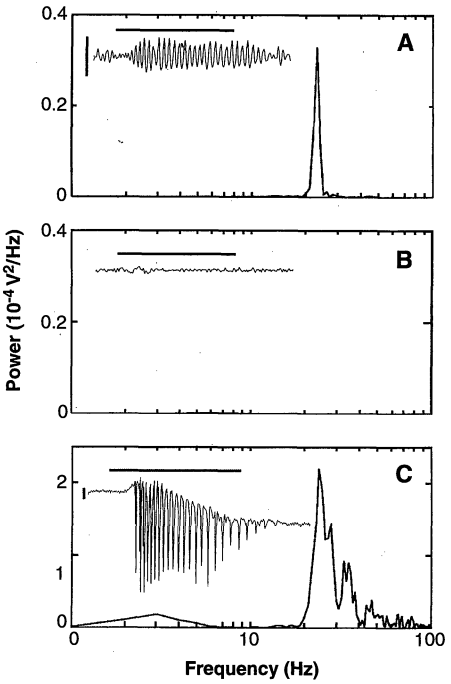


**Fig. 3.** Effect of PCT applied simultaneously to the antennal lobe and mushroom body on synchronization and LFP oscillations. (**A**) Power spectrum calculated from the LFP oscillation (example in inset) evoked by a cherry odor (horizontal bar) in an intact animal ($n$ = 20 odor presentations). A narrow peak is seen at ~24 Hz. (**B**) Superfusion of 1 mM PCT onto the brain of the same animal rapidly eliminates the LFP oscillations, as a result of the desynchronization of PNs in the antennal lobe (Fig. 2). (**C**) Seven minutes later, odor puffs now evoke bursts of large-amplitude population spikes in the mushroom body (inset), whose power spectrum also shows a peak at 24 Hz, despite the desynchronization of PNs. Calibrations (insets): horizontal, 1 s; vertical, 500 μV.

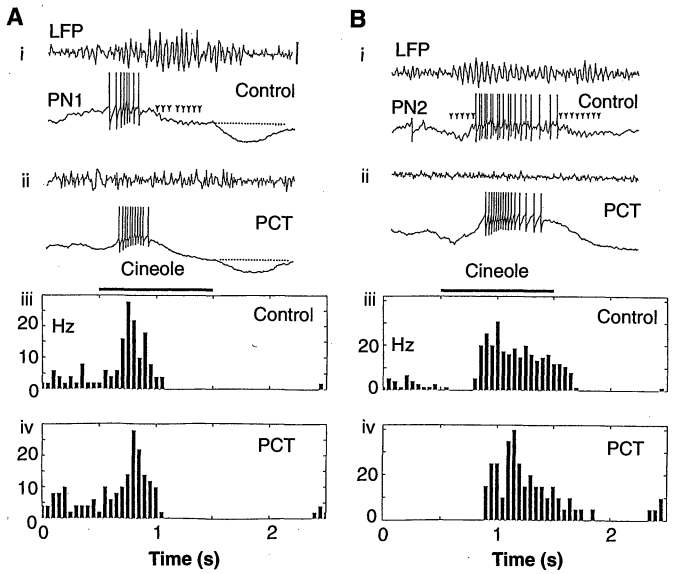


**Fig. 4.** PCT injected in the antennal lobe (**A**) (1 mM) or perfused on the brain (**B**) (5 mM) abolishes PN synchronization but does not affect odor-specific temporal response patterns of PNs. Compare the slow response patterns of two different PNs (A and B) recorded intracellularly in vivo before (i and iii) and after (ii and iv) PCT application. Although PCT abolishes the LFP oscillations (caused by synchronized PN activity) and the trains of rhythmic IPSPs visible in individual PNs [arrowheads in (i)], the timing and duration of firing of the PNs are not altered, even when periods of inhibition appear to be caused by the PCT-sensitive IPSPs. (iii and iv) Post-stimulus time histograms (instantaneous frequency in hertz) constructed from repeated presentations of the same odor before (iii) and after (iv) PCT application for these two neurons. Trial numbers: Aiii, 10; Aiv, 10; Biii, 15; Biv, 4. Bin size, 50 ms. (A) and (B) are from different animals. PN spikes are clipped. Calibrations: horizontal (i to iv), 1 s; vertical: 200 μV (LFP); 10 mV (PN).

The existence of distinct but compatible oscillatory mechanisms in the antennal lobe and mushroom body suggests that they are cooperative means to optimize synchronization and information transfer. Electrical stimulation of the lateral olfactory tract in rat piriform cortex slices evokes damped field-potential oscillations at a frequency similar to the normal bulbar input (*24*). Models of piriform cortex suggest that its networks can, in principle, be made to oscillate at this frequency by way of appropriate and realistic intrinsic recurrent connections (*25*). These data thus suggest that similar cooperative mechanisms may operate in the mammalian and locust olfactory systems.

Most importantly, the odor-specific temporal firing patterns of PNs do not depend on LN-mediated PCT-sensitive inhibition. They may result from slower antennal lobe network dynamics, possibly as a result of different inhibitory mechanisms (*26*) or temporal structuring of the olfactory receptor responses, or both. This independence of mechanisms for temporal patterning and synchronization of neural ensembles thus provides a tool to desynchronize odor-coding assemblies without otherwise altering their spatiotemporal composition. Hence, it is now possible to test, in vivo, the importance of synchronization for odor perception and memory formation.

## REFERENCES AND NOTES


1. C. M. Gray, *J. Comput. Neurosci.* **1**, 11 (1994).
2. G. Laurent, *Trends Neurosci.*, in press.
3. W. Singer and C. M. Gray, *Annu. Rev. Neurosci.* **18**, 555 (1995); A. K. Engel *et al.*, *Trends Neurosci.* **15**, 218 (1992).
4. J. G. R. Jefferys, R. D. Traub, M. A. Whittington, *Trends Neurosci.* **19**, 202 (1996).
5. E. D. Adrian, *J. Physiol. (London)* **100**, 459 (1942); W. J. Freeman, *Science* **133**, 2058 (1961); *J. Neurophysiol.* **31**, 349 (1968); M. Satou, *Prog. Neurobiol.* **34**, 115 (1990); K. Mori and Y. Yashihara, *ibid.* **45**, 585 (1995).
6. W. Rall *et al.*, *Exp. Neurol.* **14**, 44 (1966).
7. G. Laurent and M. Naraghi, *J. Neurosci.* **14**, 2993 (1994); G. Laurent and H. Davidowitz, *Science* **265**, 1872 (1994); G. Laurent, M. Wehr, H. Davidowitz, *J. Neurosci.* **16**, 3837 (1996); G. Laurent, *Neuron* **16**, 473 (1996); M. Wehr and G. Laurent, *Nature*, in press.
8. Seventy-seven adult, nonanesthetized locusts of both sexes were taken from a crowded colony and immobilized with one antenna intact as described (*7*). A window was cut open on the dorsal region of the head to gain access to the brain, which was subsequently desheathed after softening with crystals of protease type XIV (Sigma). The brain was superfused with locust saline at room temperature. Intracellular recordings were made from the soma or dendrites of local and projection neurons in the antennal lobe by means of glass micropipettes with a dc resistance of 80 to 150 megohm when filled with 3 or 0.5 M K acetate. Intracellular staining was carried out by iontophoretic injection of cobalt hexamine (6% aqueous solution), with 0.5-s, 0.5- to 2-nA pulses at 1 Hz. Histology and intensification were carried out as described [J. P. Bacon and J. S. Altman, *Brain Res.* **138**, 359 (1978)]. Airborne odors (monomolecular and blends) were puffed onto one antenna as described (*7*). Local field potentials were recorded with saline-filled patch pipettes (1- to 2-μm tips) from the mushroom body calyx.
9. W. J. Freeman, in *Olfaction, a Model System for Computational Neuroscience*, J. L. Davis and H. Eichenbaum, Eds. (MIT Press, Cambridge, MA), pp. 225–249.
10. Physiological evidence that LN depolarization can lead to PN inhibition has been provided for *Manduca sexta* [T. A. Christensen *et al.*, *J. Comp. Physiol.* **173A**, 385 (1993)]. Evidence that transmitter release from LNs to PNs does not require sodium action potentials corroborates results in the turtle olfactory bulb, where depolarized mitral cells can inhibit themselves by a reciprocal synapse with granule cells, even in the presence of tetrodotoxin, a sodium channel blocker [C. E. Jahr and R. A. Nicoll, *J. Physiol. (London)* **326**, 213 (1982)].
11. K. MacLeod and G. Laurent, data not shown.
12. B. Leitch and G. Laurent, *J. Comp. Neurol.* **373**, 487 (1996). We found direct synaptic contacts between GABA-reactive profiles (LN to LN), between non–GABA-reactive profiles (PN to PN), and between GABA- and non–GABA-reactive profiles (LN to PN and PN to LN), indicating that LNs also inhibit each other, that PNs likely excite each other, and that PNs excite LNs.
13. A small volume (~1 pl, measured before injection into the brain by injection in a drop of oil) of a selected drug was pressure-injected into the antennal lobe or mushroom body calyx with a picopump (43 experiments). The mechanical effect of injection was usually small, allowing maintained intracellular impalement of PNs. We checked that drug diffusion was restricted to the selected neuropils (probably because of efficient glial barriers surrounding the antennal lobe and mushroom body calyx) by using injections of identical volumes of cobalt hexamine. Drugs (diluted in saline) used were ionotropic GABA receptor blockers [picrotoxin (PCT, Sigma; final concentration, 0.1 to 10 mM, $n$ = 32 experiments), gabazine (SR-95531, Research Biochemical Co.; 0.1 to 10 mM, $n$ = 6), and bicuculline methiodide (BMI, Sigma; 5 to 7.5 mM, $n$ = 5)]. Of these, picrotoxin was the most effective, causing a complete block of oscillations at a bath concentration of 100 μM. Gabazine was less effective (complete block of oscillations at 5 mM). Bicuculline was totally ineffective, even at high concentrations (*15*). Other evidence suggests that histamine is an inhibitory neurotransmitter in the brain of crustaceans [B. J. Claiborne and A. I. Selverston, *J. Neurosci.* **4**, 708 (1984); T. McClintock and B. W. Ache, *Proc. Natl. Acad. Sci. U.S.A.* **86**, 8137 (1989)] and insects [R. C. Hardie, *Nature* **339**, 704 (1989)]. We thus tested the effectiveness of cimetidine (H2 receptor blocker, Sigma; 1 to 10 mM, $n$ = 7) and pyrilamine (H1 receptor blocker, Sigma; 1 to 12 mM, $n$ = 7) in blocking odor-evoked LFP oscillations. Although attenuating effects could be observed (cimetidine > pyrilamine), they always required much higher concentrations (several millimolar) than with picrotoxin. Because the insect histamine receptor channel is, like the insect ionotropic GABA receptor, a ligand-gated chloride channel, the effect of histamine receptor blockers might have been due to nonspecific binding to the GABA receptor channels. We therefore focus here only on the specific effects of picrotoxin.
14. Electrophysiological data (PN and LFP) were digitized post hoc from Digital Audio Tape with LabVIEW software and an NBMI016L interface (National Instruments, Austin, TX). Sliding cross-correlations were calculated piecewise over 200-ms-long windows shifted progressively in steps of 100 ms over each data set (simultaneous LFP and PN recordings) with the use of Matlab (*The Math Works*) as described (*7*). The cross-correlations in Fig. 2 are each constructed by averaging the cross-correlations calculated from each pair over $n$ presentations of the odor (A: $n$ = 20; B: $n$ = 23; C: $n$ = 16; D: $n$ = 14; 1-s puffs at 0.1 Hz). The structure of these functions indicates the great consistency of the synchronization between PN and LFP (Fig. 2, A, C, and D). Because cross-correlations were performed on continuous data (LFP and membrane potential), the large variations of potential caused by PN action potential waveforms needed to be weighted down for pictorial representation. We thus artificially eliminated all PN action potentials before cross-correlation analysis (spikes clipped to ~5 mV, traces band-pass filtered at 5 to 100 Hz with no phase shift), resulting in a continuous signal of amplitude, timing, and shape similar to the subthreshold synaptic waveform underlying each action potential. The periodic structure of cross-correlations calculated with the full-spike waveform was identical, except for the increased dynamic range of the cross-correlation function, rendering the pictorial display of small modulations in the function impossible (saturated at low or high amplitude).
15. Bicuculline methiodide (BMI), another vertebrate $GABA_A$ receptor antagonist, is also ineffective on most inhibitory synapses in insects but has some blocking effects on inhibition in the brain of the moth *M. sexta* [B. Waldrup, T. A. Christensen, J. G. Hildebrand, *J. Comp. Physiol.* **161A**, 23, 1987]. BMI had no effect on the odor-evoked oscillations at concentrations as high as 7.5 mM.
16. Anti-GABA immunocytochemistry on the PN axon bundle that runs between antennal lobe and mushroom body revealed about 830 axons that were all negative for GABA (*12*). The inhibitory inputs received by KCs during odor responses (*7*) must therefore originate elsewhere. They could be from feedback inhibitory neurons activated by KCs or from feedforward inhibitory neurons excited by the PNs.
17. Although LFP spectra in these conditions were usually centered on the same peak frequency, they were often broader, showed a greater variance of peak frequencies from trial to trial, and contained substantial power at higher frequencies, including peaks at harmonics of the fundamental. The reason for this change in spectral composition probably resides in the different nature of LFP signals before and during PCT application to the mushroom body. Before PCT application, LFPs are close to sinusoidal and result mainly from synaptic currents caused in the dendrites of KCs, few of which produce action potentials (*7*). After PCT application, LFPs probably result mainly from coherent and suprathreshold activity of KCs (note the asymmetrical shape and the amplitude of these bursts) and thus contain active components caused by spike-generating currents.
18. F. W. Shürmann, *Exp. Brain Res.* **19**, 406 (1974). The neurotransmitter or neurotransmitters expressed by KCs are presently unknown.
19. KCs do not express natural intrinsic oscillatory properties, as revealed by intracellular current injection in vivo (*7*). Because odors normally evoke suprathreshold responses in relatively few KCs and because the (intracellularly recorded) responses of KCs to an odor often comprise an early and maintained inhibitory component (*7*), odor-evoked KC inhibition likely results, at least in part, from a feedforward circuit.
20. Although olfactory bulb circuits appear to contain more neuronal subtypes than the insect antennal lobe, their fundamental design is markedly similar [J. G. Hildebrand, *Proc. Natl. Acad. Sci. U.S.A.* **92**, 67 (1995); J. Boeck *et al.*, in *Chemosensory Information Processing*, D. Schild, Ed. (Springer-Verlag, Berlin, 1990), pp. 201–227; G. M. Shepherd, *Neuron* **13**, 771 (1994)].
21. W. W. Lytton and T. J. Sejnowski, *J. Neurophysiol.* **66**, 1059 (1991); P. Bush and T. J. Sejnowski, *Comput. Neurosci.* **3**, 91 (1996).
22. M. A. Whittington, R. D. Traub, J. G. R. Jefferys, *Nature* **373**, 612 (1995); S. R. Cobb *et al.*, *ibid.* **378**, 75 (1995).
23. M. Chaput and A. Holley, *J. Physiol. (Paris)* **76**, 551 (1980); M. Meredith, *J. Neurophysiol.* **56**, 572 (1986); A. R. Cinelli, K. A. Hamilton, J. S. Kauer, *ibid.* **73**, 2053 (1995); M. Yokoi, K. Mori, S. Nakanishi, *Proc. Natl. Acad. Sci. U.S.A.* **92**, 3371 (1995).
24. K. L. Ketchum and L. B. Haberly, *J. Neurosci.* **13**, 3980 (1993).
25. M. Wilson and J. M. Bower, *J. Neurophysiol.* **67**, 981 (1992).
26. These mechanisms might use histamine or metabotropic GABA receptor channels, or both. They could also involve soluble gases such as nitric oxide, which can probably be produced by local neurons in insects [U. Müller and E. Buchner *Naturwissenschaften* **80**, 524 (1993)] and the terrestrial mollusc *Limax maximus* [A. Gelperin, *Nature* **369**, 61 (1994)].


27. Supported by a NSF grant and Presidential Faculty Fellow Award to G.L. We thank E. M. Schuman, N. Kopell, and members of the Laurent lab for helpful discussions and comments.

6 June 1996; accepted 19 September 1996